

Photon and lepton pair production in a quark-gluon plasma^{*}

P. Aurenche

February 1, 2008

Laboratoire de Physique Théorique LAPTH¹,
BP110, F-74941, Annecy le Vieux Cedex, France

Abstract

We discuss the production of real or virtual photons in a quark-gluon plasma.

LAPTH-Conf-810/2000

^{*}Based on talks given in July 2000 at QCD 00, Montpellier, France and at ICHEP2000, Osaka, Japan

¹UMR 5108 du CNRS, associée à l'Université de Savoie

1 Introduction

It has long been thought that electro-magnetic probes *i.e.* real or virtual photons would provide a way to detect the formation of a quark-gluon plasma in ultra-relativistic heavy ion collisions. The energy distribution of the photons would allow to measure the temperature of the plasma provided the rate of production in the plasma exceeds that of various backgrounds. It is expected that this will occur in a small window in the GeV range for the energy of the photon. At lower values of the energy the rate is dominated by various hadron decay processes while at higher values the usual hard processes (those occurring in the very early stage of the collision before the plasma is formed), calculable by standard perturbative QCD methods, would dominate. In contrast to hadronic observables (or heavy quarkonia) which are sensitive to the late evolution of the plasma as well as to the re-hadronisation phase, the photons in the GeV range are produced soon after the plasma is formed and then they escape the plasma without further interaction.

We assume the plasma in thermal equilibrium (temperature T) with vanishing chemical potential. The rate of production, per unit time and volume, of a real photon of momentum $Q = (q_o, \mathbf{q})$ is

$$\frac{dN}{dtd\mathbf{x}} = -\frac{d\mathbf{q}}{(2\pi)^3 2q_o} 2n_B(q_o) \text{Im} \Pi^R_{\mu}{}^{\mu}(q_o, \mathbf{q}) , \quad (1)$$

while for a lepton pair of mass $\sqrt{Q^2}$ it is

$$\frac{dN}{dtd\mathbf{x}} = -\frac{dq_o d\mathbf{q}}{12\pi^4} \frac{\alpha}{Q^2} n_B(q_o) \text{Im} \Pi^R_{\mu}{}^{\mu}(q_o, \mathbf{q}) , \quad (2)$$

where $\Pi^R_{\mu}{}^{\mu}(q_o, \mathbf{q})$ is the retarded photon polarisation tensor. The pre-factor $n_B(q_o)$ provides the expected exponential damping $\exp(-q_o/T)$ when $q_o \gg T$. This report is devoted to the study of Π^R which contains the strong interaction dynamics of quarks and gluons in the plasma. The theoretical framework is that of the effective theory with re-summed hard thermal loops (HTL) [1].

We briefly review the status of $\text{Im} \Pi^R$ calculated up to the two-loop approximation. Some phenomenological consequences are mentioned. Then we turn to a discussion of higher loop corrections.

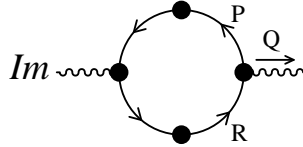


Figure 1: *One-loop contribution.*

2 The two-loop approximation

Following the HTL approach [1] one distinguishes two scales: the “hard” scale, typically of order T or larger (the energy of quarks and gluons in the plasma) and the “soft” scale of order gT where g , the strong coupling, is assumed to be small. Collective effects in the plasma modify the physics at scale gT *i.e.* over long distances of $\mathcal{O}(1/gT)$. These effects lead to a modification of the propagators and vertices of the theory and one is led to introduce effective (re-summed) propagators and vertices. This is easily illustrated with the example of the fermion propagator, $S(P)$, which in the “bare” theory is simply $1/p$ (we neglect spin complications and make only a dimensional analysis). The thermal contribution to the one loop correction $\Sigma(p)$ is found to be $\Sigma(p) \sim g^2 T^2/p$ which is of the same order as the inverse propagator when p is of order gT . The re-summed propagator $*S(P) = 1/(p - \Sigma(p))$ is then deeply modified for momenta of $\mathcal{O}(gT)$ whereas the thermal corrections appear essentially as higher order effects for hard momenta. Likewise, the gluon propagator and vertices are modified by hard thermal loops when the external momenta are soft [1]. One can construct an effective Lagrangian [2] in terms of effective propagators and vertices and calculate observables in perturbation theory.

In the one-loop approximation, the photon production rate is given by the diagram shown in fig. 1 where the symbol \bullet means that effective propagators and vertices are used. The result has been known for some time and can be expressed, in simplified notation, as [3, 4]

$$\text{Im } \Pi^R(q_o, \mathbf{q}) \sim e^2 g^2 T^2 \left(\ln\left(\frac{q_o T}{m_q^2}\right) + C\left(\frac{Q^2}{m_q^2}\right) \right) \quad (3)$$

where $m_q^2 \sim g^2 T^2$ is related to the thermal mass of the quark. One notes the presence of a “large” logarithmic term $\ln(1/g)$ dominating over a “constant term” $C(Q^2/m_q^2)$.

The two-loop diagrams are displayed in fig. 2. In principle, there are more diagrams in the effective theory but only those leading to the dominant

contribution are shown. All propagators and vertices should be effective but since the largest contribution arises from hard fermions it is enough, following the HTL strategy, to keep bare fermion propagators and vertices

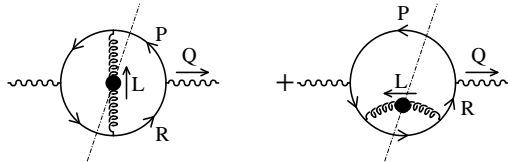


Figure 2: *The dominant two-loop contributions.*

as indicated². Only the gluon line needs to be effective since soft momentum L through the gluon line dominates the integrals. To evaluate these diagrams it is convenient to distinguish between the contribution arising from a time-like gluon ($L^2 > 0$) and a space like gluon ($L^2 < 0$). The first type leads to a contribution similar to eq. (3) and requires some care as counter-terms (not shown) eliminate the parts of the two-loop diagrams already contained in the one-loop diagrams [5]. We concentrate on the second case which in terms of physical processes corresponds to bremsstrahlung production of a photon or production in a quark-antiquark annihilation process where one of the quark is put off-shell by scattering in the plasma (see fig. 3). The result for hard photons is [6]

$$\text{Im } \Pi^R(q_o, \mathbf{q}) \Big|_{\text{brems}} \sim e^2 g^2 T^2 \quad (4\text{-a})$$

$$\text{Im } \Pi^R(q_o, \mathbf{q}) \Big|_{\text{annil}} \sim e^2 g^2 T q_0 \quad (4\text{-b})$$

The reason why these two-loop contributions have the same order as the one-loop one is due to the presence of strong collinear singularities. To calculate $\text{Im } \Pi^R$ one has to cut the propagators as indicated by the dash-dotted lines in fig. 2. In the integration over the loop hard momentum P (with P^2 , $(R + L)^2$ on shell) the denominators R^2 and $(P + L)^2$ of the un-cut fermion propagators simultaneously almost vanish when \mathbf{p} is parallel to \mathbf{q} *i.e.* in the collinear configuration. This leads to an enhancement factor of type T^2/M_{eff}^2 where the cut-off $M_{\text{eff}}^2 = m_q^2 + p(p + q_0)Q^2/q_0^2$ emerges from the calculation. For the kinematic range of concern to us here, $M_{\text{eff}}^2 \sim g^2 T^2$ so

²Note that for consistency of our approach, based on an expansion in terms of effective quantities, we keep the thermally generated mass in the hard limit of the effective propagator.

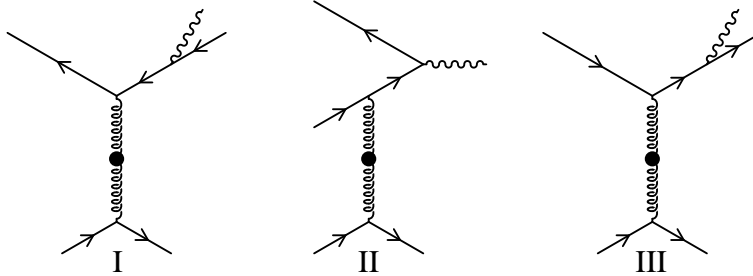


Figure 3: *Physical processes included in the diagrams of Fig. 2, in the region $L^2 < 0$. I: bremsstrahlung with an antiquark. II: $q\bar{q}$ annihilation with scattering. III: bremsstrahlung with a quark.*

that the two-loop diagram is enhanced by a factor $1/g^2$ which compensates the g^2 factor associated to the coupling of the gluon to the quarks. An interesting result of the calculation is the importance of process II of fig. 3 which grows with the energy of the photon and dominates over the other contributions when $q_0/T \gg 1$ as shown in fig. 4. Phenomenological applications of these results have been carried out and the two-loop processes have been included in hydrodynamic evolution codes to predict the rate of real photon production at RHIC or LHC [7]. It is found that the two-loop processes (especially the annihilation with scattering) lead to an increase by an order of magnitude compared to the one-loop processes. This may even have consequences for heavy ion collisions at SPS energies [8]. Several effects may reduce these over-optimistic predictions: lack of chemical equilibrium and more importantly higher order corrections as discussed next.

3 Higher order corrections

Since the one-loop and two-loop results are of the same order it is reasonable to worry about the convergence of the perturbative expansion in the effective theory! The enhancement mechanism operative at two-loop could also be at work at the multi-loop level especially in ladder diagrams, an example of which is shown in fig. 5: indeed many “small” fermion denominators appear in such diagrams which can produce a pile-up of collinear singularities. A recent study of the three-loop ladder diagram shows that [9]

$$\text{Im } \Pi^R \Big|_{3\text{-loop}} \sim \text{Im } \Pi^R \Big|_{2\text{-loop}} \times \frac{g^2 T}{l_{\min}} \quad (5)$$

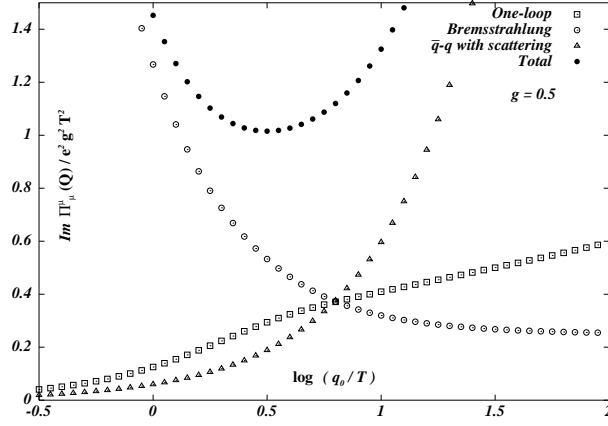


Figure 4: Comparison of various contributions to $\text{Im } \Pi_\mu^\mu(Q)$ for a hard real photon. The comparison is made for $N = 3$ colors and $N_F = 2$ flavors.

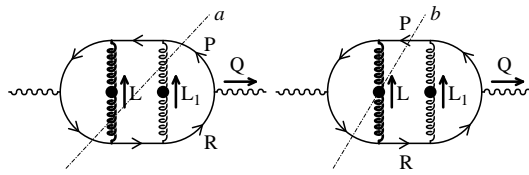


Figure 5: A ladder diagram.

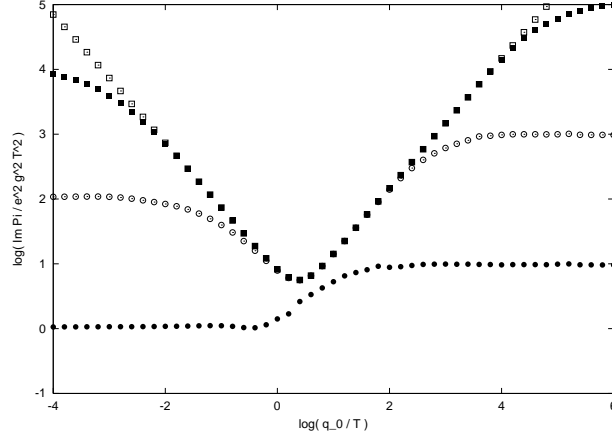


Figure 6: *Effect of the width Γ on the two-loop contributions. Each curve corresponds to a different values of Γ . From top to bottom, the ratio $\Gamma T/m_q^2$ takes the values 10^{-6} , 10^{-4} , 10^{-2} and 1.*

where l_{min} is the largest of the cut-offs:

- $l_{min}^{(1)} = M_{eff}^2 q_0 / p_0 r_0$, which is the collinear cut-off encountered above: it depends on the thermal quark mass and momentum ($p_0 \sim r_0 \sim T$) as well as on the external variables;
- $l_{min}^{(2)} = m_D \sim gT$, the Debye mass if the added gluon is longitudinal, or $l_{min}^{(2)} = m_{mag} \sim g^2 T$ if it is transverse.

For the kinematic configuration of interest, in the case of an extra longitudinal gluon one can check that $m_D \gg l_{min}^{(1)}$ and the Debye mass acts as a cut-off with the result that the three-loop contribution is suppressed by a factor g compared to the two-loop. On the contrary, for a transverse gluon, both regulators are of order $g^2 T$ (as long as $Q^2/q_0^2 < g^2$) and the three-loop diagram is of the same order as the two-loop one. One is therefore in a non-perturbative regime. The problem is similar to the magnetic mass problem pointed out by Linde in the perturbative calculation of the free energy [10], except that here it appears at leading order.

Another effect which can modify the collinear enhancement mechanism is related to the fermion damping rate. Indeed, including the damping rate on the fermion lines, will shift the pole of the propagators away from the real axis: this affects the enhancement mechanism based on the near-vanishing of the denominators. Ignoring the requirement of gauge invariance and concentrating only on the mathematical effect of shifting the poles to

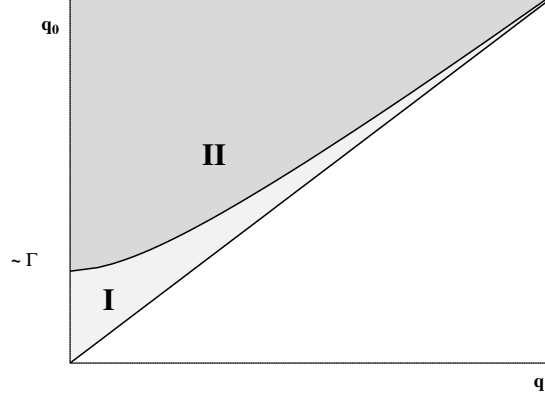


Figure 7: Boundary obtained from the condition $\hat{\Gamma} = 1$. In region I, the width is the dominant regulator of collinear singularities. In region II, the width is only a sub-dominant correction.

the complex plane one can do again the two-loop calculation with fermion propagators including the damping rate $\Gamma \sim g^2 T \ln(1/g)$. The result is intuitively simple as a regulator of the form [11]

$$\mathcal{M}_{\text{eff}}^2 = M_{\text{eff}}^2 + 4i\Gamma \frac{p_0(p_0 + q_0)}{q_0} \quad (6)$$

comes out, with M_{eff}^2 defined above. The effect of Γ on $\text{Im } \Pi^R(q_o, \mathbf{q})|_{2\text{-loop}}$ is shown on fig. 6 for the case of a real photon ($Q^2 = 0$). The region $q_o/T < 1$ is dominated by bremsstrahlung emission while the region $q_o/T > 1$ receives a contribution mainly from the annihilation with scattering process (see fig. 4). The top curve is the result obtained with a vanishingly small width. One notes the change in the q_o behaviour of $\text{Im } \Pi^R(q_o, \mathbf{q})$ as Γ increases: this is due to the different q_o dependences of the real and imaginary parts of $\mathcal{M}_{\text{eff}}^2$. For virtual photon production, one notes that the quantity $|\text{Re } \mathcal{M}_{\text{eff}}^2|$ increases with Q^2 at fixed q_o so that the ratio $\hat{\Gamma} = \text{Im } \mathcal{M}_{\text{eff}}^2 / \text{Re } \mathcal{M}_{\text{eff}}^2$, which controls the relative importance of the width, decreases. For Q^2 large enough the effect of Γ will become negligible and the two-loop calculation should be adequate. This is illustrated in fig. 7.

Equation (6) lends itself to a simple interpretation. It can be written as

$$\mathcal{M}_{\text{eff}}^2 = 2 \frac{p_0(p_0 + q_0)}{q_o} (1/\lambda_{\text{for}} + i/\lambda_{\text{mean}}) \quad (7)$$

where $\lambda_{\text{mean}} = 1/\Gamma$ is the mean free path of the quark in the plasma and $\lambda_{\text{for}} = 2p_0(p_0 + q_0)/M_{\text{eff}}^2 q_0$ can be shown to be the formation length of the photon. Then, if $\lambda_{\text{mean}} \gg \lambda_{\text{for}}$ the effect of the damping rate can be ignored and the corresponding higher order diagrams are suppressed. In the opposite case, re-scattering in the plasma modifies the two-loop result. This is equivalent to say that the Landau-Pomeranchuk-Migdal (LPM) effect [12] has to be taken into account in the calculation. Two interesting features emerge from the above discussion: 1) the LPM effect not only modifies the production of bremsstrahlung photon but also that of very hard photons emitted in the “annihilation with scattering” process as illustrated in fig. 6; 2) if the virtuality Q^2 of the hard lepton pair is large enough then one falls in the domain $\lambda_{\text{mean}} \gg \lambda_{\text{for}}$ and the perturbative calculation at two-loop is sufficient.

The problems discussed above are an illustration of a more general situation concerning thermal Green’s function with external momenta close to the light-cone [13].

The production mechanism of hard photons in the plasma is very complex. New processes appear at two-loop which considerably increase the rate of photon production calculated at one-loop. However, for real or small mass virtual photons the higher loop diagrams become important and the rate turns out to be non-perturbative. Taking into account higher order effects to obtain a quantitative estimate remains to be done.

Acknowledgments

I thank F. Gelis, R. Kobes and H. Zaraket for a fruitful collaboration on the work discussed above.

REFERENCES

1. E. Braaten, R.D. Pisarski, *Nucl. Phys. B* **337** (1990) 569; **339** (1990) 310. J. Frenkel, J.C. Taylor, *Nucl. Phys. B* **334** (1990) 199; **374** (1992) 156.
2. J.C. Taylor, S.M.H. Wong, *Nuc. Phys. B* **346** (1990) 115. E. Braaten, R.D. Pisarski, *Phys. Rev. D* **45**(1992) 1827.
3. J.I. Kapusta, P. Lichard, D. Seibert, *Phys. Rev. D* **44** (1991) 2774; R. Baier, H. Nakkagawa, A. Niegawa, K. Redlich, *Z. Phys. C* **53** (1992) 433.

4. T. Altherr, P.V. Ruuskanen, *Nucl. Phys. B* **380** (1992) 377. M.H. Thoma, C.T. Traxler, *Phys. Rev. D* **56** (1997) 198.
5. P. Aurenche, F. Gelis, R. Kobes, H. Zaraket, *Phys. Rev. D* **60** (1999) 076002.
6. P. Aurenche, F. Gelis, R. Kobes, H. Zaraket, *Phys. Rev. D* **58** (1998) 085003.
7. D.K. Srivastava, *Eur. Phys. J. C* **10** (1999) 487; M.G. Mustafa, M.H. Thoma, *Phys. Rev. C* **62** (2000) 014902.
8. D.K. Srivastava, B. Sinha, nucl-th/0006018.
9. P. Aurenche, F. Gelis, H. Zaraket, *Phys. Rev. D* **61** (2000) 116001.
10. A.D. Linde, *Phys. Lett. B* **96** (1980) 289.
11. P. Aurenche, F. Gelis, H. Zaraket, hep-ph/0003326, to appear in *Phys.Rev. D*.
12. L.D. Landau, I.Ya. Pomeranchuk, *Dokl. Akad. Nauk. SSR* **92** (1953) 735; A.B. Migdal, *Phys. Rev.* **103** (1956) 1811.
13. F. Gelis, hep-ph/0007087.